Modeling and Reduction of Crosstalk on Coupled Microstrip Line Structures and Multichip Modules: An FDTD Approach

Mubashir Rizvi[1] and Joe LoVetri

Department of Electrical Engineering, The University of Western Ontario, London, Ontario N6A 5B9, Canada. E-mail: joe@gauss.engga.uwo.ca

Received February 1, 1995; revised May 11, 1995.

ABSTRACT

The finite difference time domain modeling technique is used to model the near end and far end crosstalk on coupled microstrip structures used in multichip modules. The lines are terminated in lumped resistors which closely, but not exactly, match the lines. One line is excited by a Gaussian voltage pulse produced by a Thévenin equivalent voltage source. It is shown that adding dielectric strips in the substrate below the conducting lines will reduce the peak crosstalk by as much as 80%. Eight different configurations are modeled consisting of dielectric strips with different dielectric constant combinations. All configurations are modeled with and without a metal case in order to make sure that the crosstalk reduction persists when the structure is enclosed in a metallic enclosure (this would be the case for multichip modules). The results show that using dielectric strips with the smallest possible dielectric constant reduces crosstalk the most.

I. INTRODUCTION

Technological advancements in the fabrication of electronic devices are required for faster signal propagation and higher device densities. The successful achievement of these objectives is critically challenged by the EMI constraints of the system. Enclosing the circuitry in a metal package, as in the case of multichip modules (MCMs) and MMIC devices, further degrades the RF circuit performance because of the onset of package resonances and more, in general, due to the interactions of electromagnetic fields produced by the signal propagating in the electronic circuitry and due the package itself (see refs. 1 and 2). An understanding of these complex electromagnetic field interactions is therefore essential for the success of a system, either packaged or otherwise.

In this study we choose to analyze a microstrip-based structure (described below) due to its popularity in industry as a basis for creating complex systems for very high frequency and microwave applications. Since microstrips require simple technology they are very well-suited for production purposes. Semiconductors, dielectrics, resonators, antennas, and active devices may be easily implanted on a substrate.

Though microstrip-based structures are easy to fabricate, they are extremely difficult to analyze theoretically. This is because their structure presents three kinds of complexities.

1. The electromagnetic fields extend over air and one (or more) dielectric substrate(s), so

[1]Currently with Bell Northern Research, Mail Stop 005, 21 Richardson Side Road, Kanata, Ontario K2K 2C1, Canada.

CCC 1050-1827/96/010058-11

the waves on a transmission line cannot be considered a pure TEM mode.
2. Thin conducting strips require inhomogeneous boundary conditions along the air-dielectric surface.
3. At high frequencies the circuitry may radiate. If the structure is enclosed within a metallic box, the waves reflect back to produce coupling and resonances.

A number of techniques have been proposed for increasing the device densities [3–7]. This article proposes an alternative approach based on selective substrate compensation. The key to the design process is to use dielectric strips in the substrate beneath the conducting lines to reduce the effects of intersignal coupling (or crosstalk) which presents one of the prime obstacles in reducing the overall design size. The effect is demonstrated in the time domain.

The most common material used as the substrate in MCMs is ceramic. There are three main reasons why ceramic is being used as a substrate for designing MCMs in the industry.

1. The thermal characteristics of ceramic allow for faster heat dissipation.
2. The adhesive properties of ceramic allow other materials to be "patched" in with it.
3. The resemblance of ceramic to silicon (from a properties standpoint).

Results presented in this article show that the greatest reduction in peak crosstalk is achieved when Teflon (epsilon = 2.2) is used as the material for the dielectric patches beneath the conductors. In general it is not possible to use a homogeneous substrate made of Teflon only. This is so because, although the use of Teflon as a substrate will improve the EMI/EMC situation, there are other issues pertaining to manufacturability which will not allow it. Foremost in this regard are the inferior adhesive properties of Teflon.

The question as to whether or not the proposed dielectric compensation scheme presented in this paper is manufacturable must also be addressed. Current MCM technologies offer a variety of approaches to MCM fabrication and module packaging. The most promising MCM technologies currently available are:

1. MCM-L: high density laminated PC board.
2. MCM-C: cofired ceramic.
3. MCM-D: deposited organic thin film on a silicon, ceramic metal base.
4. MCM-Si: silicon substrate with a silicon dioxide (SiO_2) dielectric.
5. MCM-HDI: high density interconnect technology.

A review of the manufacturing process used for MCM's is detailed in ref. 8. Our proposed design is not just manufacturable, and therefore practical to implement, but current MCM technology is utilizing the advantages of multiple materials in the substrate for numerous other purposes [9]. For example, the thermal constraints related to high-speed signal propagation are a great limitation in the MCM design process. These constraints are greatly reduced when multiple layers of substrates are used [10]. The use of patches of different material have also been used as "caps" to avoid copper corrosion and diffusion into the overlaying dielectric layer of thin film structures [11]. The notion of multimaterial substrate is also being used in the water-scale integration (WSI) technology [12].

II. SUBSTRATE COMPENSATED MICROSTRIP STRUCTURE

The microstrip structure we consider in this article is shown in Figure 1. As can be seen the structure consists of two conducting microstrips above an inhomogeneous substrate. The two dielectric strips which have relative dielectric constants of ε_1 and ε_2 are placed beneath the microstrips and are implanted in the substrate having a relative dielectric constant of $\varepsilon = 10$ (ceramic). The width of the dielectric strips is 4 mm, the width of the microstrips is 3 mm, and the spacing between the microstrips is 4 mm. All units in the figure are millimeters, unless otherwise stated.

From an electrical point of view, the passive line (T2) is terminated on both ends by lumped resistors having a resistance value of $R = 50\ \Omega$. The far end of the active line (T1) is also terminated by $R = 50\ \Omega$ and the near end of the active is excited by a Thévenin equivalent voltage source, $V(t)$, having a Thévenin resistance of $R_s = 7\ \Omega$. These resistance values do not provide an impedance match for the lines but are typical of input/output impedances encountered in digital designs.

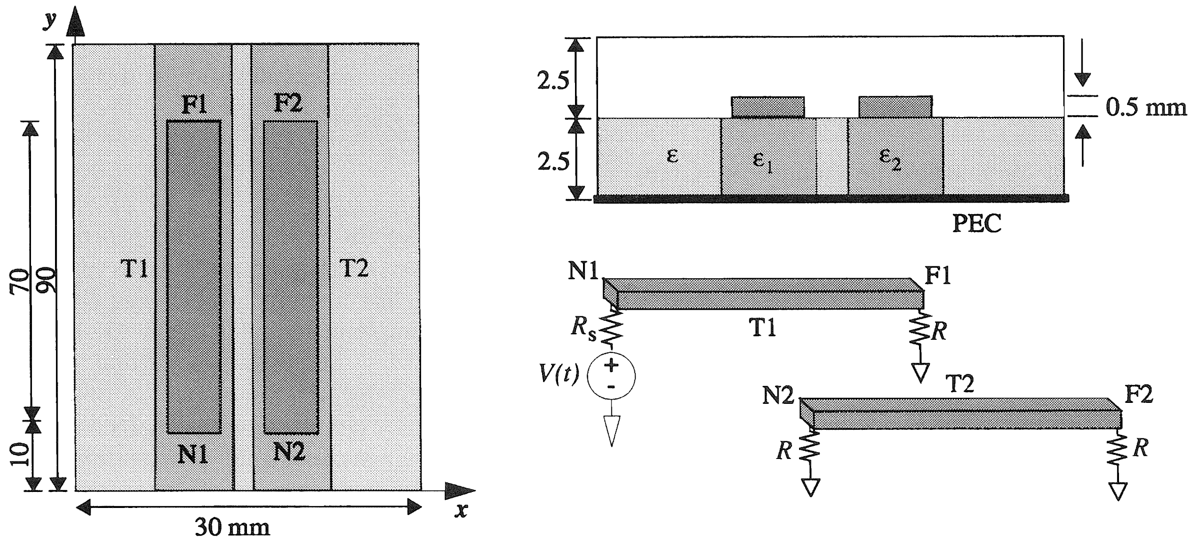

Figure 1. Top view (left), side view (top right), and electrical configuration (bottom right).

In the analysis which follows three different materials are used for the dielectric strips. The choice of these materials have been made to encompass the range of relative primitivities for the materials commonly used in industry for the manufacture of PCBs, MCMs, and IC packages. Nine different cases were considered based on the three dielectric materials. A description of these nine cases is detailed in Table I.

The sets of numerical experiments were conducted twice—once for the structure described in Figure 1 and then repeated for the scenario when the circuitry described in Figure 1 was packaged in a perfectly conducting case. Thus, the package was simulated by imposing tangential electric fields equal to zero on all faces of the computational domain boundary.

From a lumped circuit point of view the microstrip structure presented in Figure 1 tries to take advantage of the proportionality relationship between the capacitance and the crosstalk voltage appearing on the passive line. The key to the design process is to use dielectric strips which effectively reduce the mutual capacitance between the strips. Since capacitance is also proportional to the relative permittivity of the material, a decrease in crosstalk voltage may be possible by using a material with lower relative permittivity.

III. NUMERICAL ANALYSIS OF THE PROBLEM

Simple microstrip structures are "open" structures in which the field extends all the way to infinity. In practice these structures are enclosed within metal boxes and the electromagnetic waves are reflected from the walls of the enclosure. These waves then interact with the enclosed circuitry producing suprious coupling. The understanding and mitigation of these effects is the key to increase the device density. Simple microstrip models do not consider wave excitations and therefore cannot make predictions about the phenomena.

Various computational methods are available in the literature, however, most of them are restricted to special geometries or are not applicable due to the lack of generality [13–16, 18–20]. Most analysis models are based on a static or quasistatic approach yielding lumped equivalent circuits for gaps, bends, steps, and junctions. These

TABLE I. Nine Cases of Ceramic Substrate Compensation (ε = 10.0)

	Case								
	1	2	3	4	5	6	7	8	9
ε_1	10.0	10.0	4.7	2.2	2.2	2.2	4.7	4.7	10.0
ε_2	4.7	2.2	10.0	10.0	2.2	4.7	4.7	2.2	10.0

methods are restricted to thin substrates because they neglect the fringing effect and radiation. An extensive review of these methods is available [21].

The spectral domain approach is often used in the computation of propagation characteristics of coupled lines (see ref. 15). However, this method can only be applied to planar structures and losses are introduced by a perturbational calculation. Knowledge of the Green's function is required by other methods, such as the method of moments (MoM) (see ref 16), and are therefore restricted to planar or symmetrical structures. The finite element method (FEM) is flexible and a wide scope of problems may be approximated by employing it. However mesh generation is a challenge and suppression of spurious modes is another major task. [17].

A relatively simple but powerful numerical technique is the discretization of the differential form of Maxwell's equations in space and time via the finite-difference time-domain (FDTD) method [22–29]. This is the technique employed in this study and a brief overview of the method as well as a description of the capabilities of our code is now given.

Yee's Algorithm: Brief Overview

First presented in 1966 by K. S. Yee [22], the FDTD technique is attractive because of its simplicity, computational efficiency, direct physical interpretation, and accuracy. It has been employed in a wide range of applications. These include electromagnetic wave propagation and scattering problems [23, 24, 30, 31], aperture coupling [32–34], electromagnetic interaction with biological tissues [36–38], electromagnetic pulse coupling [27, 28, 39, 40], and microwave circuit and design problems [41, 42].

An explicit central differencing scheme, the "leap-frog scheme," is used to discretize Maxwell's two curl equations. As a result, 16 independent sets of spatially and temporally discrete interleaved electric and magnetic fields are created. Eliminating all but one of these independent sets of fields, as shown in Figure 2, results in what is known as the FDTD or Yee's algorithm.

In the algorithm, the field components are positioned at offset locations about a unit cell of the grid (see Fig. 2). Also the electric and magnetic field components are evaluated at alternate half-time steps.

Features of Our FDTD Code

Since most practical electromagnetic problems involve regions with different constitutive properties and scatterers in the domain of interest, the practical implementation of Yee's algorithm into a general purpose code requires careful attention to detail in order to not degrade computational efficiency when making provisions to include these capabilities. Research into specific techniques for including lumped circuit elements into the FDTD mesh have been recently addressed [43, 44]. Our code currently has the following features: an optimized rectangular grid FDTD engine written in the standard C language; first and second order Mur absorbing boundary conditions (ABCs); and the capability to insert lumped elements at any point in the grid and across as many cells as is required. The types of elements are: inductors, capacitors, resistors, and Thévenin/Norton equivalent circuits with current and voltage sources defined by a function of time (typically Gaussian).

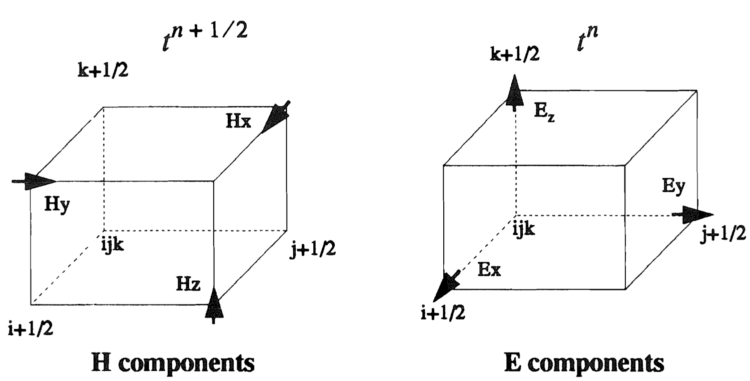

Figure 2. Computational molecule.

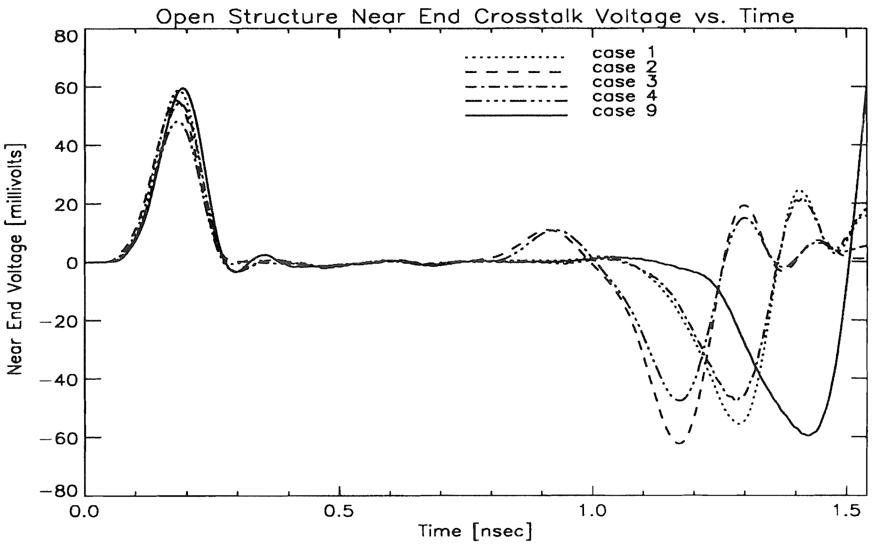

Figure 3. Open structure near end crosstalk, cases 1, 2, 3, 4, and 9.

Analysis of Microstrip Problem: Computational Information

A Gaussian voltage pulse containing appreciable frequency components up to 1.2 GHz was used to excite the active line. The frequency of the waveform used was therefore typical of the "fast" waveforms used in the industry today.

A uniform grid with a cell size of $0.5 \times 0.5 \times 0.5$ mm was used. The geometry of the microstrip structure considered translates to a computational domain of size approximately equivalent to $(50)^3$ cells. The time increment was set to the Courant limit to satisfy the stability criterion and limit numerical dispersion. The code was executed for 2000 time steps. The processing time on an HP Model 715/75 workstation with 64 Mb RAM was about 2 hours.

The Thévenin voltage source as well as the resistors were modeled by using $6 \times 1 \times 5$ cells along the x, y, and z directions, respectively. This "spreading" of voltages and resistances over a number of cells was used after experimenting with other configurations. It was found that this configuration provides the most effective modeling accuracy and oscillations and ringing are re-

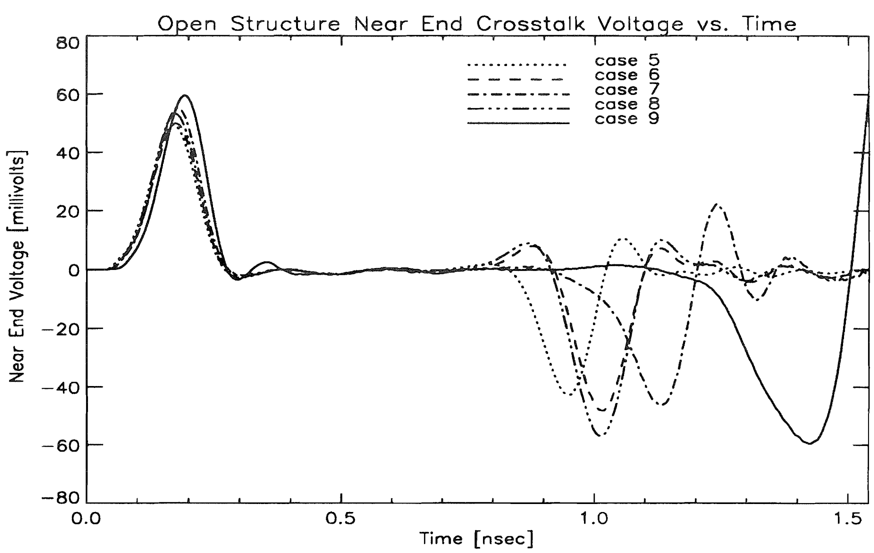

Figure 4. Open structure near end crosstalk, cases 5, 6, 7, 8, and 9.

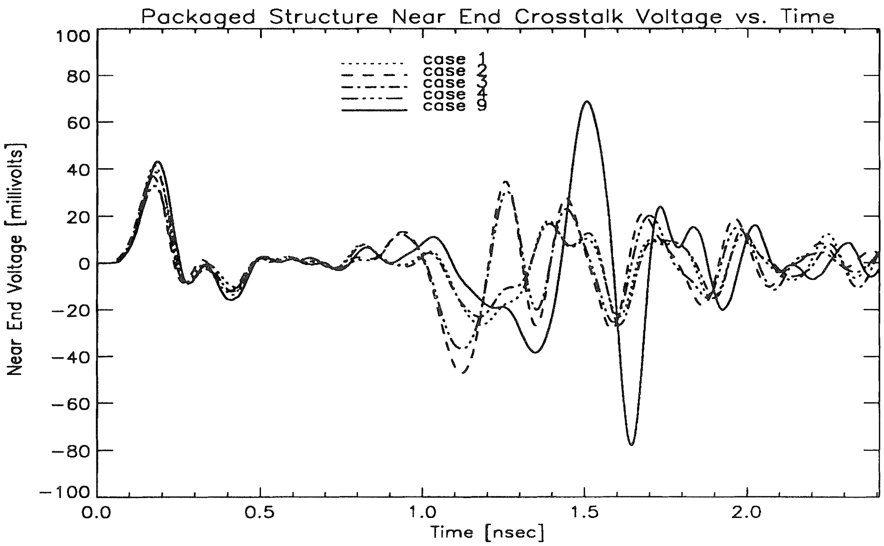

Figure 5. Packaged structured near end crosstalk, cases 1, 2, 3, 4, and 9.

duced to a minimum. The source as well as the resistors were oriented along the z-axis.

IV. RESULTS AND DISCUSSION

The computational results of the near end and far end crosstalk for all the 9 cases of Table I for both the open structure and the packaged structure are shown in Figures 3–10.

As can be seen from these figures the different cases show a wide variation in the near end and far end crosstalk voltage waveforms. From a digital circuitry point of view the peak value of the time domain crosstalk waveform is critical. Thus we have tabulated the percent reduction in the peak value of the negative and positive near end and far end crosstalk voltage waveforms in Tables II and III for the open microstrip and packaged microstrip structure, respectively. The reduction is relative to the peak value of the waveform for case 9, that is, the homogeneous case where no dielectric strips were placed under the microstrips. Case 9 was also plotted as a solid curve in all the figures for easy reference.

As can be seen from the figures and the tables,

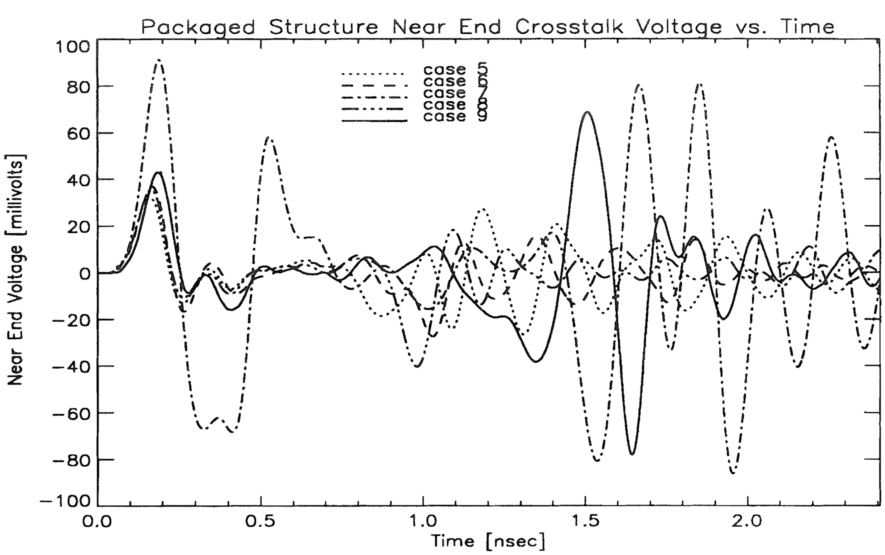

Figure 6. Packaged structure near end crosstalk, cases 5, 6, 7, 8, and 9.

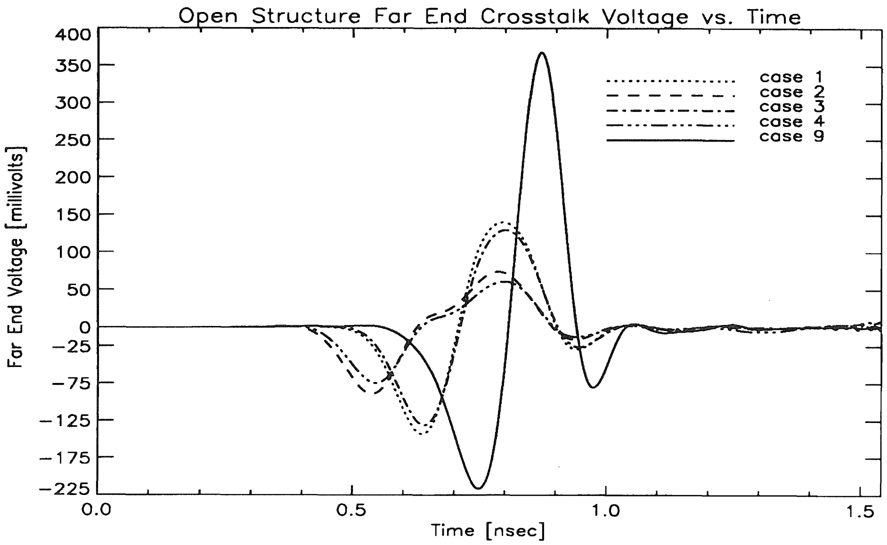

Figure 7. Open structure far end crosstalk, cases 1, 2, 3, 4, and 9.

except for case 2 in the open structure and case 7 in the packaged structure, all cases resulted in a substantial reduction in the peak crosstalk. We also note the different crosstalk resulting from unsymmetrical structures. For example, cases 1 and 3, as well as 2 and 4 are equivalent asymmetrical structures but the cases differ as to which of the lines is excited. It can be seen that reducing the self-capacitance of the active line alone will generally reduce the crosstalk more than reducing the self-capacitance of the passive line alone.

In general if both the near end and far end crosstalk are of concern then it can be seen that the best scenario occurs when we decrease the dielectric constant of both dielectric strips as much as possible, that is, case 5.

V. CONCLUSION

The FDTD technique has been used to analyze open and packaged coupled microstrip structures where dielectric strips are inserted beneath the conducting microstrips. By using dielectric strips of low dielectric constant, lower than the substrate, a significant reduction in the far end and

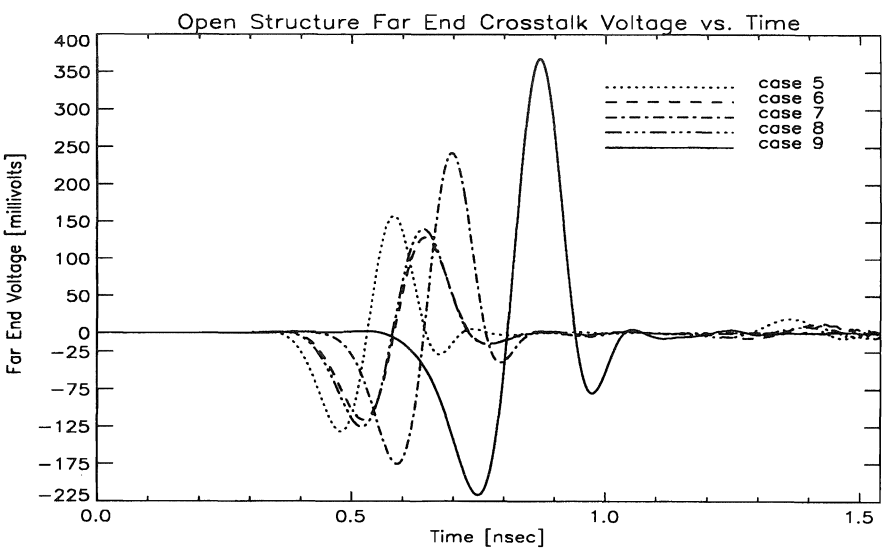

Figure 8. Open structure far end crosstalk, cases 5, 6, 7, 8, and 9.

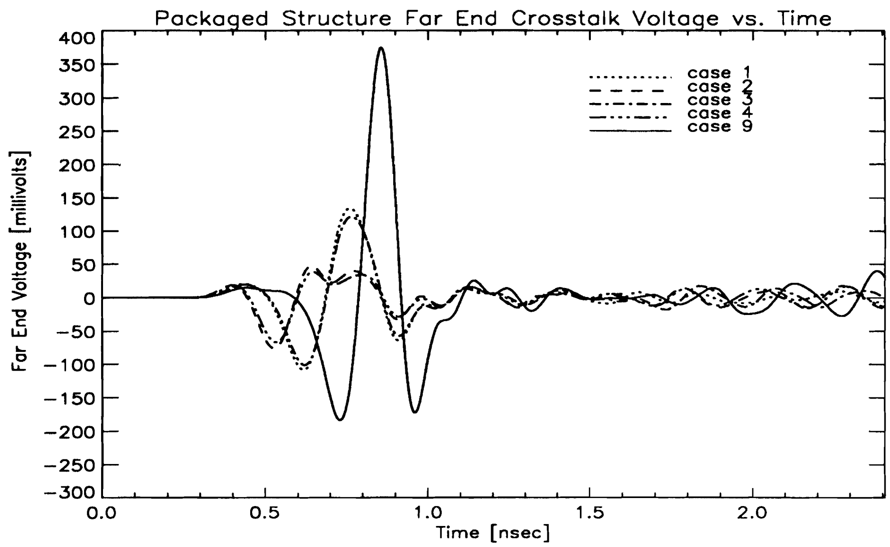

Figure 9. Packaged structure far end crosstalk, cases 1, 2, 3, 4, and 9.

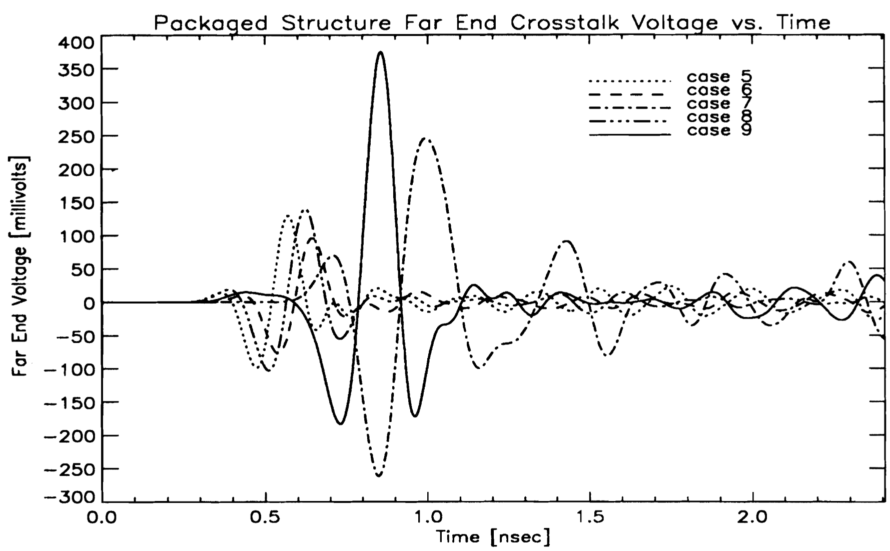

Figure 10. Packaged structure far end crosstalk, cases 5, 6, 7, 8, and 9.

TABLE II. Open Microstrip Structure

Case	ε_1	ε_2	Near end crosstalk, percentage (%) decrease in:		Far end crosstalk, percentage (%) decrease in:	
			Positive peak	Negative peak	Positive peak	Negative peak
1	10	4.7	1.12	6.69	61.96	33.91
2	10	2.2	7.02	−4.59	79.90	58.76
3	4.7	10.0	8.56	19.74	64.74	39.40
4	2.2	10.0	19.13	20.24	83.45	65.54
5	2.2	2.2	17.09	28.26	57.16	39.03
6	2.2	4.7	16.00	19.34	65.03	46.49
7	4.7	4.7	7.20	22.03	34.03	19.02
8	4.7	2.2	10.58	4.55	61.89	42.04
9	10.0	10.0	0	0	0	0

TABLE III. Structure Packaged in a Metal Enclosure

			Near end crosstalk, percentage (%) decrease in:		Far end crosstalk, percentage (%) decrease in:	
Case	ε_1	ε_2	Positive peak	Negative peak	Positive peak	Negative peak
1	10	4.7	40.02	65.86	64.23	40.83
2	10	2.2	46.19	39.51	87.53	58.54
3	4.7	10.0	43.96	65.91	67.59	44.73
4	2.2	10.0	52.25	52.81	89.87	63.53
5	2.2	2.2	52.71	65.86	65.66	46.22
6	2.2	4.7	46.95	64.81	74.48	58.07
7	4.7	4.7	−32.61	−10.39	34.56	−42.43
8	4.7	2.2	48.38	48.18	62.85	43.89
9	10.0	10.0	0	0	0	0

near end crosstalk has been achieved. It has been demonstrated that there exists a potential to increase the device density by using this technique of substrate compensation. It has also been demonstrated that full-wave solvers may be used as "drawing boards" to optimize and analyze faster and denser electronic systems.

REFERENCES

1. J. J. Burke and R. W. Jackson, "A Simple Circuit Model for Resonant Mode Coupling in Packaged MMIC's," *1991 Int. IEEE MTT-S Symp. Dig.*, pp. 1221–1224.
2. R. W. Jackson, "Removing Package Effects from Microstrip Moment Method Calculations," *1992 Int. IEEE MTT-S Symp. Dig.*, pp. 1225–1299.
3. J. P. Glib and C. A. Balanis, "Asymmetric, Multi-Conductor Low-Coupling Structures for High-Speed, High-Density Digital Interconnects," *IEEE Trans. MTT*, Vol. 39, No. 12, December 1991, pp. 2100–2106.
4. J. P. Glib and C. A. Balanis, "Transient Analysis of Distortion and Coupling in Lossy Coupled Microstrips," *IEEE MTT-S Int. Microwave Symp. Dig.* (Dallas, TX), 1990, pp. 641–644.
5. L. Carin and K. J. Webb, "Isolation Effects in Single- and Dual-Plane VLSI Interconnects," *IEEE Trans. MTT*, Vol. 38, April 1990, pp. 396–404.
6. S. Seki and H. Hasegawa, "Analysis of Crosstalk in Very High-Speed LSI/VLSI's Using a Coupled Multi-Conductor MIS Microstrip Line Model," *IEEE Trans. MTT*, Vol. 32, pp. December 1984, 1715–1720.
7. J. P. Glib and C. A. Balanis, "Pulse Distortion on Multilayer Coupled Microstrip Lines," *IEEE Trans. MTT*, Vol. 37, October 1989, pp. 1620–1628.
8. S. D. Kadakia, T. E. Donovan, D. Gupta, and H. Bhatia, "Advanced Design and Modeling for Manufacturability of a Hybrid MCM Package," *IEEE Trans. Components, Packaging and Manufacturing Tech.* B: *Advanced Packaging*, Vol. 17, No. 2, May 1994, pp. 170–174.
9. J. Jean and T. K. Gupta, "Design of Low Dielectric Glass + Ceramics for Multilayer Ceramic Substrate," *IEEE Trans. Components, Packaging and Manufacturing Tech.* B: *Advanced Packaging*, Vol. 17, No. 2, May 1994, pp. 228–233.
10. J. F. McDonald, H. T. Lin, N. Majid, and S. Darbal, "Low Temperature Processing—the Route to MultiChip Packaging," *Proceedings of IPC 31st Annual Meeting*, April 18–22, 1988, Hollywood, FL.
11. R. S. Patel, T. A. Wassick, and C. Y. Ralston, "Metal Capping of MCM Thin Film Features using a Laser," *IEEE Trans. Components, Packaging and Manufacturing Tech.* B: *Advanced Packaging*, Vol. 17, No. 2, May 1994, pp. 264–268.
12. I. P. Jalowiecki, "The WASP3 Monolithic-WSI Massively Parallel Processor," *IEEE Trans. on Components, Packaging, and Manufacturing Tech.* B: *Advanced Packaging*, Vol. 17, No. 2, May 1994, pp. 318–323.
13. T. Itoh, (ed.), *Numerical Techniques for Microwave and Millimeter Wave Passive Structures*. New York, Wiley, 1989.
14. E. G. Farr, C. H. Chan, and R. Mittra, "A Frequency-Dependent Coupled Mode Analysis of Microstrip Lines with Application to VLSI Interconnection Problems," *IEEE Trans. on MTT*, Vol. 34, February 1986, pp. 307–310.
15. R. H. Jansen, "The Spectral-Domain Approach for Microwave Integrated Circuits," *IEEE Trans MTT*, Vol. 33, October 1985, pp. 1043–1056.
16. L. P. Dunleavy and P. B. Katehi, "A Generalized Method for Analyzing Shielded Thin Microstrip Discontinuities," *IEEE Trans. MTT*, Vol. 36, December 1988, pp. 1758–1766.

17. W. Schroeder and I. Wolff, "The Origin of Spurious Modes in Numerical Solutions of Electromagnetic Field Eigenvalue Problems," *IEEE Trans. MTT*, Vol. 42, No. 4, April 1994, pp. 644–653.
18. T. Angkaew, M. Matsuhara, and N. Kumagai, "Finite-Element Analysis of Waveguide Modes: A Novel Approach that Eliminates Spurious Modes," *IEEE Trans. MTT*, Vol. 35, February 1987, pp. 117–123.
19. A. R. Djordjevic, T. K. Sarkar, and R. F. Harrington, "Time-Domain Response of Multiconductor Transmission Lines," *Proc. IEEE*, Vol. 75, June 1987, pp. 743–754.
20. S. Nam, H. Ling, and T. Itoh, "Characterisation of Uniform Microstrip Line and its Discontinuities Using the Time-Domain Method of Lines," *IEEE Trans. MTT*, Vol. 37, December 1989, pp. 2051–2057.
21. R. K. Hoffmann, *Handbook of Microwave Integrated Circuits*. Artech House, Dedham, MA, 1988.
22. K. S. Yee, "Numerical Solution of Initial Boundary Value Problems Involving Maxwell's Equations in Isotropic Media," *IEEE Trans. AP*, Vol. 14, No. 5, May 1966, pp. 302–307.
23. A. Taflove and K. R. Umashankar, "Review of FD-TD Numerical Modeling of Electromagnetic Wave Scattering and Radar Cross Section," *IEEE Proc.*, Vol. 77, May 1989, pp. 682–699.
24. A. Taflove and K. R. Umashankar, "The Finite-Difference Time-Domain Method for Numerical Modeling of Electromagnetic Wave Interactions," *Electromagnetics*, Vol. 10, January 1990, pp. 105–126.
25. D. H. Choi and W. Hoefer, "The Finite-Difference Time-Domain Method and Its Application to Eigenvalue Problems," *IEEE Trans. MTT*, Vol. 34, August 1986, pp. 1464–1469.
26. G. C. Liang, Y. W. Liu, and K. K. Mei, "Full-Wave Analysis of Coplanar Waveguide and Slotline Using the Time-Domain Finite-Difference Method," *IEEE Trans. MTT*, Vol. 37, December 1989, pp. 1949–1957.
27. K. S. Kunz and K. Lee, "A Three-Dimensional Finite Difference Solution of the External Response of an Aircraft to a Complex Transient EM Environment: Part I—The Method of Its Implementation," *IEEE Trans. EMC*, Vol. 20, May 1978, pp. 328–333.
28. K. S. Kunz and K. Lee, "A Three-Dimensional Finite Difference Solution of the External Response of an Aircraft to a Complex Transient EM Environment: Part II—Comparison of Predictions and Measurements," *IEEE Trans. EMC*, Vol. 20, May 1978, pp. 333–341.
29. J. F. Lee, R. Palandech, and R. Mittra, "Modeling Three-Dimensional Discontunities in Waveguides Using Non-orthogonal FDTD Algorithm," *IEEE Trans. MTT*, Vol. 40, February 1992, pp. 346–352.
30. P. A. Tirkas and K. R. Demarest, "Modeling of Thin Dielectric Structures Using the Finite-Difference Time-Domain Technique," *IEEE Trans. AP*, Vol. 39, September 1991, pp. 1338–1344.
31. C. L. Britt, "Solution of Electromagnetic Scattering Problems Using Time Domain Techniques," *IEEE Trans. AP*, Vol. 37, September 1989, pp. 1181–1192.
32. A. Taflove, K. Umashankar, B. Beker, F. Harfoush, and K. Yee, "Detailed FD-TD Analysis of Electromagnetic Fields Penetrating Narrow Slots and Lapped Joints in Thick Conducting Screens," *IEEE Trans. AP*, Vol. 36, February 1988, pp. 247–257.
33. K. R. Demarest, "A Finite-Difference Time-Domain Technique for Modeling Narrow Apertures in Conducting Scatters," *IEEE Trans. AP*, Vol. 35, July 1987, pp. 826–831.
34. D. J. Riley and C. D. Turner, "Hybrid Thin-Slot Algorithm for the Analysis of Narrow Apertures in Finite-Difference Time-Domain Calculations," *IEEE Trans. AP*, Vol. 38, December 1990, pp. 1943–1950.
35. J. A. Shaw, H. D. Durney, and D. A. Christensen, "Computer-Aided Design of Two-Dimensional Electric-Type Hyperthermia Applicators Using the Finite Difference Time-Domain Method," *IEEE Trans. Biomed. Eng.*, Vol. 38, September 1991, pp. 861–870.
36. P. J. Dimbylow, "Finite Difference Time-Domain Calculations of Absorbed Power in the Ankle for 10–100 MHz Plane Wave Exposure," *IEEE Trans. Biomed. Eng.*, Vol. 38, May 1991, pp. 423–428.
37. D. M. Sullivan, "Mathematical Methods for Treatment Planning in Deep Regional Hyperthermia," *IEEE Trans. MTT*, Vol. 39, February 1991, pp. 864–872.
38. J. Gilbert and R. Holland, "Implementation of Thin-Slot Formalism in the Finite-Difference EMP Code TREDII," *IEEE Trans. Nucl. Sci.*, Vol. 28, December 1981, pp. 4589–4591.
39. R. Holland and L. Simpson, "Finite-Difference Analysis of EMP Coupling to Thin Struts and Wires," *IEEE Trans. EMC*, Vol. 23, May 1981, pp. 88–97.
40. R. Holland, L. Simpson, and K. S. Kunz, "Finite Difference Analysis of EMP Coupling to Lossy Dielectric Structures," *IEEE Trans. EMC*, Vol. 22, August 1980, pp. 328–333.
41. J. F. Lee, R. Palandech, and R. Mittra, "Modeling Three-Dimensional Discontinuities in Waveguides Using Non-Orthogonal FDTD Algorithm," *IEEE Trans. MTT*, Vol. 40, February 1992, pp. 346–352.
42. X.Zhang, J. Fang, K. K. Mei, and Y. Lui, "Calculations of the Dispersive Characteristics of Microstrips by the Time-Domain Finite-Difference Method," *IEEE Trans. MTT*, Vol. 36, February 1988, pp. 263–267.

43. W. Sui, D. A. Christensen, and C. H. Durney, "Extending the Two-Dimensional FD–TD Method to Hybrid Electromagnetic Systems with Active and Passive Lumped Elements," *IEEE Trans. MTT*, Vol. 40, April 1992, pp. 724–730.

44. V. A. Thomas, M. E. Jones, M. Piket-May, A. Taflove, and E. Harrigan, "The Use of SPICE Lumped Circuits as Sub-Grid Models for FDTD Analysis," IEEE Microwave and Guided Wave Letters, Vol. 4, No. 5, May 1994, pp. 141–143.

BIOGRAPHIES

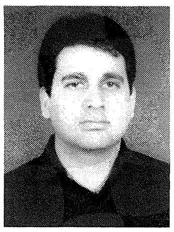

Mubashir Rizvi was born in Karachi, Pakistan in 1968. He received the BSc degree from N.E.D. University in Engineering and Technology, Karachi, Pakistan and the MSc degree in electrical engineering from the University of Western Ontario, London, Ontario, Canada in 1991 and 1995, respectively. His research interests include computational electromagnetics modeling, high speed circuits and system design.

Joe LoVetri was born in Enna, Italy, in 1963. He received the BSc (with distinction) and MSc degrees, both in electrical engineering, from the University of Manitoba in 1984 and 1987, respectively. From 1984 to 1986 he was an EMI/EMC engineer at Sperry Defence Division in Winnipeg, Manitoba. From 1986 to 1988 he held the position of TEMPEST engineer at the Communications Security Establishment in Ottawa. From 1988 to 1991 he was a research officer at the Institute for Information Technology of the National Research Council of Canada. He received the PhD degree in electrical engineering from the University of Ottawa in 1991. He is currently an associate professor in the Department of Electrical Engineering at the University of Western Ontario where he has been since 1991. His main interests lie in time domain computational electromagnetics. His specific research interests are in time domain modeling of linear and nonlinear electromagnetic waves and in topological modeling of practical electromagnetic interference and compatibility problems.